lncCRLA Enhanced Chemoresistance in Lung Adenocarcinoma That Underwentepithelial-mesenchymal Transition

Weili Min
Xi'an Jiaotong University
Liangzhang Sun
Xi'an Jiaotong University
Xiao Gao
Xi'an Jiaotong University
Shuqun Zhang
Xi'an Jiaotong University
Yang Zhao (szhaoy@126.com)
Second affiliated hospital of Xi'an Jiaotong University

Research

Keywords: EMT,chemotherapy resistance, lung adenocarcinoma, lncRNA

Posted Date: June 17th, 2020

DOI: https://doi.org/10.21203/rs.3.rs-35582/v1

Abstract

Background

EMT confers increased metastatic potential andtheresistance to chemotherapiesto cancer cells.However, the precise mechanisms of EMT-related chemotherapy resistance remain unclear.

Methods

Anticancer effects were determined by MTT, soft agar, cell cycle, propidium iodide and Annexin V analysis. The effect of drugs on tumor growth was assessed using patient-derived xenograft model and nude mice model.Morphology of tumor cells were observed by phase contrast microscopy. Proteins interactions were tested by western blot and coimmunoprecipitation. Immunohistochemistry and LNA ISH were performed to determine protein and lncRNA expression. Candidate lncRNA was screened out by microarray.

Results

c-Src-mediated Caspase-8 phosphorylationessential for EMT in lung adenocarcinoma cell linespreferentially occurs in cells with themesenchymal phenotype,resultingin chemoresistance tocisplatin plus paclitaxel in patients with resectable lung adenocarcinoma and a significantly worse5-yearPFS. Cisplatin killedlung adenocarcinoma cells regardless of Caspase-8. Paclitaxel-triggered necroptosis in lung adenocarcinoma cells was dependent on the phosphorylation or deficiency ofCaspase-8, during which FADDinteracted with RIPK1 to activateRIPK1/RIPK3/MLKL signaling axis. Accompanied with c-Src-mediated Caspase-8 phosphorylation to trigger EMT, a novel lncRNA named lncCRLA was markedly upregulated andinhibited RIPK1-induced necroptosis byimpairingRIPK1-RIPK3 interaction via binding to the intermediate domain of RIPK1. Dasatinibmitigatedc-Src-mediated phosphorylationof Caspase-8-induced EMT and enhanced necroptosis in mesenchymal-like lung adenocarcinoma cells treated with paclitaxel, while c-FLIP knockdown predominantly sensitized the mesenchymal-like lung adenocarcinoma cells to paclitaxel+dasatinib.

Conclusions

c-Src-Caspase-8 interaction initiatesEMT and chemoresistance viaCaspase-8 phosphorylation and lncCRLA expression, to which the dasatinib/paclitaxel liposome+siFLIPregimen was lethal.

Highlights

Highlights: l c-Src-mediated Caspase-8 phosphorylation in lung adenocarcinoma was required forEMT to facilitate chemoresistance to paclitaxel. l Caspase-8 phosphorylation or deficiency induced the paclitaxel-mediated necroptosis in lung adenocarcinoma. l Activation of lncRNA-related chemotherapy resistance in lung adenocarcinoma (lncCRLA) during c-Src-Caspase-8-induced EMT inhibited RIPK1-induced

necroptosis. l A novel therapeutic agent, paclitaxel liposome encapsulating siRNA specific for c-FLIP combined with clearly sensitized the mesenchymal-like lung adenocarcinoma cells.

Background

lnboth the United States and P.R. China,lung cancer is not only the leading cause of cancer deathby far but also the second leading cause of death from any cause after heart diseasebased on calculations from published data [1, 2]. Non-small-cell lung cancer (NSCLC) accounts for approximately 85% of lung cancers with a markedly increased incidence of lung adenocarcinoma [3]. The 5-year overall survival rate for lung adenocarcinoma is only 17% because, in a startlingly high proportion of patients with lung adenocarcinoma, the disease has already metastasizedat the initial diagnosis or recurs after initial surgery or radiotherapy [4, 5]. Lung adenocarcinoma is generally incurable because it will either have an intrinsic resistance to chemotherapy or develop acquired resistance after an initial response [6, 7]. Therefore, identifying molecular determinants of the resistance to chemotherapy in lung adenocarcinoma is necessary to improve its clinical efficacy.

Despite significant advances in diagnosing and treating lung adenocarcinoma, metastasis persists as a barrier to successful treatmentand the main cause of cancer-related death [8-10]. Epithelial-mesenchymal transition (EMT), wherein epithelial cells depolarize, lose their cell–cell contacts, and gain an elongated, fibroblast-like morphology, is a potential mechanism by which tumor cells acquiremetastatic features [11, 12]. The prometastatic role of EMT in various human cancers was recently challenged by the research groups of Kari R. Fisher and Xiaofeng Zheng, who both stated that EMT was not a rate-limiting step for metastasis but rather inadvertently conferred resistanceto antiproliferativedrugs such as gemcitabine [6, 13]. Notwithstanding, EMT-induced resistance to antitumor drugs remains an integral characteristic of lung adenocarcinoma. We observed that phosphorylation ofCaspase-8 by c-Src induced both EMT through c-Src overactivation and resistance to chemotherapy through necroptosis [14]. Hence, the mechanism by which phosphorylated Caspase-8 confers resistance to chemotherapy appearedto be worth pursuing.In our study, c-Src-mediated Caspase-8 phosphorylationessential for the EMT in lung adenocarcinoma cell lineswas preferential forthemesenchymal phenotype, leading to chemoresistance tocisplatin plus paclitaxel in patients with resectable lung adenocarcinoma. Cisplatin rendered lung adenocarcinoma cells susceptible to death regardless of Caspase-8, while the paclitaxel-triggered necroptosis in lung adenocarcinoma cells was dependent on the phosphorylation or deficiency of Caspase-8.During this necroptosis activation, FADD interplayed with RIPK1 to activate theRIPK1/RIPK3/MLKL signaling axis. Concomitantwith c-Src-mediated Caspase-8 phosphorylation to trigger EMT, a brand-new lncRNA, named lncCRLA, was markedly upregulatedto inhibit RIPK1-induced necroptosis byimpairingof the RIPK1-RIPK3 interaction viabinding to the intermediate domain of RIPK1. Dasatinib, a c-Src inhibitor, impaired c-Src-mediated phosphorylation of Caspase-8-induced EMT and enhanced necroptosis in paclitaxel-treated mesenchymal-like lung adenocarcinoma cells. Intriguingly,c-FLIP knockdown predominantly sensitized the mesenchymal-like lung adenocarcinoma cells to paclitaxel+dasatinib.

Methods

Ethics approval and consent to participate

The procedures of this study, including 7 references, were approved by the Ethics Committee of the Second Affiliated Hospital of Xi'an Jiaotong University.The experiments were performedupon receiving written consent from each subject.The study methodologies conformed to the standards set by the Declaration of Helsinki.

Reagents and drugs

Paclitaxel (Bristol-Myers Squibb) was purchased from Sigma for cell culture and animal studies at concentrations of 100 nM, 200 nM, and 400 nM. An original solution of cisplatin (Pfizer) at a concentration of 1 M was stored at 4°C and freshly dissolved in culture medium before use. Dasatinib (Sprycel, Bristol-Myers Squibb) was dissolvedin dimethyl sulfoxide (DMSO) and used at a final concentration of 10^{-6} M. z-VAD-fmk (50 mM) and z-IETD-fmk (50 mM) were obtained from Alexis Biochemicals. 3-Methyladenine (3-MA, 1 mg/10 ml) was purchased from InvivoGen. Necrostatin-1 (nec-1, 10 mM) was generously gifted by Chen Huang from the Department of Cell Biology, Xi'an JiaotongUniversity, Shaanxi Province, P.R. China.

Cell culture, DNA/shRNA transfection and stable cell line generation

Lung adenocarcinoma cell lines, including A549, National Cancer Institute (NCI)-H522 and H23, were kind gifts from Chen Huang from the Department of Cell Biology, Xi'an JiaotongUniversity, Shaanxi Province, P.R. China. H1395, H1437, H1573, H920, H2935, H1650, H1299, H2030, H2405, H647 and H838 cells were purchased fromAmerican Type Culture Collection (ATCC) and cultured in RPMI 1640 supplemented with 10% fetal bovine serum (FBS, HyClone) and penicillin/streptomycin/L-glutamine (Sigma). The cell lines in our study were authenticated by short tandem repeat (STR) analysis. To observe the morphologic features of EMT, we cultured cells for 5 days on fibronectin (10 μg/ml)-coated dishes. Cells were assayed for expression and viability following treatment with reagents or drugs at 2 days after attachment tothe fibronectin-coated dishes. Knockdown of RIPK1, FADD, c-FLIP, Caspase-8, c-Src or lncCRLA was performed using lentivirus-delivered short hairpin RNAs (shRNAs) constructed by GenePharma (shRNAs targeting c-FLIP and lncCRLAcorresponded to the siRNAs below; Shanghai, China). Following lentiviral transfection, stable cell lineswere selected via culturing in the presence of 500 μg/ml G418 (Gibco). The open reading frames of genes of interest, including wild-type Caspase-8, wild-type RIPK1, death domain-deleted RIPK1, intermediate domain-deleted RIPK1, kinase domain-deleted RIPK1, c-Src, and constitutively active c-Src (Src Y527F), were cloned into the MSCV-IRES-zeo plasmid with a hemagglutinin (HA) tag to allow the expression of HA-tagged proteins. The subsequent DNA was transfected into packaging cells. Virus-containing supernatants were removed, and debris was pelleted by centrifugation. Target cells were cultured in virus-containing supernatants for 48 hr before selection for a stable cell line with 10 mg/ml zeocin (Invitrogen) for 14 days.

Results

c-Src-induced Caspase-8 phosphorylation wasrequired for EMT in lung adenocarcinoma cell lines.

In lung adenocarcinoma, the molecular characteristics of EMT could be divided into mesenchymal, epithelial, and intermediate phenotypes based on the expression of E-cadherin (E-cad) and Vimentin (Vim) [15]. We distinguished our lung adenocarcinoma cell lines as having epithelial ormesenchymal properties (described as epithelial-like and mesenchymal-like cells, respectively). Prior work showedthat phosphorylation ofCaspase-8 at tyrosine 380 (p-Casp8) by c-Src enhances c-Src activation (p-Src) and triggers EMT[14, 16, 17]. Thus, it was likely that p-Casp8 could functionas a biomarker for EMT in lung adenocarcinoma.We initially investigated the expression levels of c-Src and Caspase-8 in lung adenocarcinoma cells, which showedubiquitous expressionof both proteins; however,Caspase-8 expression was absent in H522 cells (Figs 1A and 1B). p-Casp8 was present in the mesenchymal-likelung adenocarcinoma cell lines with lower E-cad levels and higher Vim levels (Fig S1A), whereas no p-Casp8 was observed in the epithelial-like cell lines with higher E-cad levels and lower Vim levels (Fig S1B). There was remarkably lower c-Srcexpression in the epithelial-like cell lines than in the mesenchymal-like cell lines (Figs 1A and 1B). A549 cells transfected with control shRNA and H522 cells with ectopic expression ofCaspase-8 presentedthe mesenchymal-likemorphologywith E-cad downregulation and Vim upregulation (A549+Control/H522+Casp8: mesenchymal-like;Figs S1C, 1C and 1D), whereas A549 cells with c-Src/Caspase-8 knockdown andH522 cells transfected with control vector presented epithelial properties (A549+Casp8/Src shRNA and H522+Control: epithelial-like;Figs S1C, 1C and 1D).Taken together,c-Src-induced Caspase-8 phosphorylation was required for EMT in lung adenocarcinoma cell lines.

To further clarify the role of c-Srcin EMT, we ectopicallyexpressedc-Src in epithelial-like lung adenocarcinoma cell lines with Caspase-8 expression (H1395, H1437, H1573, H1693, and H1568). The molecular and morphological characteristics in cells were more mesenchymal-like; these changes were concomitant withmarkedly increased levels of p-Casp8 and p-Src in the epithelial-likelung adenocarcinoma cell lines transfected with c-Src(Figs 1E, 1F and S1D). Furthermore, upregulation of c-Src induced more aggressive behavior in the epithelial-like cell lines(Figs 1G, S1E and S1F). It was noteworthy that c-Src was mildlyactivated in H522 cells lacking Caspase-8. The results suggested that the expression level of c-Src was associated with its basicactivity to initiate Caspase-8 phosphorylation in lung adenocarcinoma.

c-Src-induced Caspase-8 phosphorylation was associated with themesenchymal phenotype and contributed to chemoresistance in lung adenocarcinoma.

As the antiapoptotic role of p-Casp8 in several human tumors has been described[16], we soughtto uncover the underlying mechanism by which p-Casp8-induced EMT restricted the clinical efficacy of the TP regimen in lung adenocarcinoma. It was a tremendouschallenge to assess the epithelial/mesenchymal status of tumor tissues due to the heterogeneity in the diverse domains of the tumor. According to our outcomes and a prior report [15, 17], Vim and E-cad were confirmed as

appropriate biomarkers to predict the epithelial/mesenchymal properties oflung adenocarcinoma tissues. We initially assessed the levelsof p-Casp8, Vim and E-cadthrough immunohistochemistry (IHC) in 40 patients with operable lung adenocarcinoma(Figs 2A, 2B and 2C; Table 1). p-Casp8 was associated with upregulated Vim and downregulated E-cad expression and with mesenchymal-like properties(Figs S2A, S2B and S2C), indicating that p-Casp8 could serveas a biomarker for EMT in lung adenocarcinoma tissues.

We next investigated the relationship between p-Casp8 leveland the response rate to neoadjuvant chemotherapy in patients with resectable lung adenocarcinoma. A total of 109 patients were divided into p-Casp8-positive (n = 52) and p-Casp8-negative (n = 57) groups (Table S1). Patients with p-Casp8-positive lung adenocarcinoma presented significantly lower complete response (CR) and partial response (PR) rates following 2 neoadjuvant cycles ofTP regimen(Fig 2D). In addition to thelower response rate to the TP regimen, the p-Casp8-positive cohort exhibited a remarkably worse 5-year PFS ($p< 0.05$, Fig 2E). Next, we recruited 20 patients with metastatic lung adenocarcinoma to examine thelevels of p-Casp8. As shown in Table S2, patients with p-Casp8-negative lung adenocarcinoma exhibiteda better response to the TP regimen than did patients with p-Casp8-positive lung adenocarcinoma. Based on CT images, there was a significant reduction in lesion size in the p-Casp8-negative group (Figs S2D and S2E). Then, 7 pairs of pretreatment and posttreatment biopsies were acquired, andwe detected markedly increasedp-Casp8 following two cycles of the TP regimen (FigS2F). Moreover, the proportion of p-Casp8-positive cells was sharply increasedfollowing TP regimen administration (Fig S2G). Taken together, the results showed thatin lung adenocarcinomas,p-Casp8 wasassociated with mesenchymal-like properties and contributed to disease progression by increasing the resistance to the TP regimen.

c-Src-mediated Caspase-8 phosphorylation inhibited cell death of lung adenocarcinoma through thepaclitaxel-triggered necroptosis during EMT.

Next, we sought to determine the underlying mechanism for the difference in response to the TP regimen in p-Casp8-positive and p-Casp8-negative lung adenocarcinoma. A549 cells were stably transfected with lentiviral control, Caspase-8, or c-Src shRNA (A549+Control: mesenchymal-like;A549+Caspase-8/c-Src shRNA: epithelial-like). Cisplatin caused A549 cell death in the time- and concentration-dependent manner regardless of c-Src or Caspase-8expression (Fig 3A). Cisplatin might not contribute to resistance to the TP regimen in p-Casp8-positivelung adenocarcinoma. Comparing with the mesenchymal-like A549 cells, the antitumor efficacy of paclitaxel in A549 cells transduced with c-Src shRNA wasmost potent and was dependent on the intervention time anddrug concentration (Fig 3B), while Caspase-8 knockdown inA549 cells strikingly yielded a marked increase in paclitaxel-mediated cell death (Fig 3B). These data were further supported by *in vivo* xenograft and *in vitro* colony assays (Figs S3A and S3B). Then, we analyzed the response to the TP regimen in the lung adenocarcinoma tissues fromp-Casp8-negative patients, who were divided into two groups according to IHC testing of Caspase-8 and c-Src:Casp8(+)c-Src(-) (n = 20)and Casp8(-)c-Src(+) (n = 37), (Fig S3F). The response to the TP regimen in Casp8(+)c-Src(-) patients was significantly superior to that in Casp8(-)c-Src(+) patients (Figs S3G and S3H). It indicated that

Caspase-8 yieldedmore antitumor activities relative to phosphorylated or lacking Caspase-8in response to paclitaxel treatment in lung adenocarcinoma.

Paclitaxel interfereswith mitotic spindle dynamics to induce an extended G2/M arrest,which can lead to cell death [18]. Consistently, paclitaxel significantlyenhanced G2/M arrest of A549 cells (Fig S3C). To decipher the paclitaxel-triggered cell death mechanism in lung adenocarcinoma, the inhibitors specific for RIPK1-induced necroptosis (nec-1), Caspase-8-induced apoptosis (z-IETD-fmk), pan-Caspase-induced apoptosis (z-VAD-fmk), and autophagy (3-MA) were applied. As shown in Figure 3C, paclitaxel committed approximately 70% of c-Src-silenced A549 cells to death as indicatedby a marked increase in the number of Annexin V-positive cells (apoptotic cells); this activitywas completely blocked by either z-IETD-fmkor z-VAD-fmk alone (Figs 3C and S3D). Prior work reported that blocking Caspase-8-induced apoptosis led to cell death dependenton RIPK1 and RIPK3, which was defined as necroptosis following sensing death [19, 20]. Consistently, paclitaxel gave rise to a marked increase in the proportion of propidium iodide (PI)-positive cells (necrotic cells) in A549 cells transduced with Caspase-8 shRNA (Fig 3C), that was prevented by the addition of nec-1 (Fig S3D). Notably, the mesenchymal-like A549 cells (A549+Control) with Caspase-8 phosphorylation were resistant to paclitaxel-induced cell death;however, treatment with nec-1 restored a smaller amountof cell death compared with that in A549 cells transduced with Caspase-8 shRNA (Figs 3B, 3C and S3D). The type of celldeath, apoptosis or necroptosis, in the paclitaxel-treated A549 cells was identified by observing apoptotic or necrotic featuresunder an electron microscope (Fig 3D).

To extend our notion, we examined the mesenchymal-like and the epithelial-like lung adenocarcinoma cell lines. Paclitaxel was more lethal to the epithelial-like cell lines except for H522 cells which naturally lacked Caspase-8 (Fig. S3E). Nec-1 blocked the paclitaxel-induced cell death of mesenchymal-like cells (Fig 3E), whereas z-IETD-fmk restored the viability of the epithelial-like cells (Fig S3E). With the epithelial-like properties, Caspase-8-deficient H522 cells showed cell death similar toA549 cells transduced with Caspase-8 shRNA (Fig S3E). In addition, autophagy might not influence either cisplatin- or paclitaxel-induced cell death (Fig 3C). Taken together, Caspase-8 phosphorylation or knockdown initiated the necroptosis of lung adenocarcinoma under paclitaxel treatment, whereas the mesenchymal-like A549 cells with control shRNA had the considerable resistance to paclitaxel.

Our previous study revealed that phosphorylated Caspase-8 by c-Src overactivated c-Src to phosphorylate E-cadherin phosphorylated by RNF43-initiated E-cadherin ubiquitination to maintain EMT in lung adenocarcinoma [17].To dissect the relationship between EMT and resistance to chemotherapy, we stably transfected H522 cells with control vector, Caspase-8 holoprotein or constitutively active c-Src(Src Y527F) (Fig S3I)[21] and A549 cells with control or RNF43 shRNA (Fig S3J), in which H522 cells expressing Caspase-8/Src Y527F and A549 cells with RNF43 knockdown exhibited the mesenchymal-like properties [17]. RNF43 knockdown impaired EMT without influencing thec-Src-Caspase-8 interaction and promoted amarked increase in necroptotic cell deathin A549 cellstreatedwithpaclitaxel (Fig S3H). Intriguingly, the transfection of Src Y527F and Caspase-8 into H522 cells facilitated EMT and obviously attenuated

paclitaxel-induced cell death(Fig 3K). Collectively, these data suggest that the induction of EMT based on c-Src-Caspase-8 increased the resistance of lung adenocarcinoma to paclitaxel.

FADD interacted with Caspase-8, c-FLIP and RIPK1 to induce cell death signaling following paclitaxel treatment.

Next, we determined the molecular mechanisms underlying the antitumor efficiency of paclitaxel. Paclitaxel triggered the apoptotic cleavage of Caspase-8 in c-Src-silenced A549 cells (Fig 4A). After we labeledtumor cells with [^{32}P]-orthophosphate, RIPK1, RIPK3 and MLKL were phosphorylated in A549 cells stably transfected with Caspase-8 shRNA treated with paclitaxel (Fig 4A), whereasA549 cells transfected with control shRNA exhibited a reduction in RIPK1, RIPK3, and MLKL phosphorylation(Fig 4A). H522 cells with control vector and ectopic expression of Caspase-8 presented a similar outcome as A549 cells under paclitaxel treatment (Fig S4A). To determine whether RIPK1 activation played an important role in the paclitaxel-induced necroptosis of lung adenocarcinoma, we applied the RIPK1 inhibitor, nec-1 to paclitaxel-treated A549 and H522 cells. Nec-1 was able to block RIPK1/RIPK3/MLKL activation in A549 and H522 cells with Caspase-8 deficiency or phosphorylation (Figs 4B and S4B). In the absence of Caspase-8, c-Src overactivation via the expressionof constitutively active c-Src(Src Y527F) in H522 cells exhibitingEMT attenuatedthe necroptotic RIPK1/RIPK3/MLKL signaling(Fig S4A). Collectively, it was plausible that themesenchymal state of lung adenocarcinoma cells yielded the resistance to paclitaxel-induced necroptosis.

Previous workelucidatedthat FADDboundto Caspase-8, cellular FLICE (FADD-like IL-1β-converting enzyme)-inhibitory protein (long) (c-FLIP) and RIPK1 through death effector domains (DEDs) orthe death domain (DD) to trigger alternative cell death pathways, apoptosis or necroptosis [14, 22]. We investigated whether FADD was necessaryto induce lung adenocarcinoma cell death through its interaction with Caspase-8, c-FLIP and RIPK1. FADD deletion had no effect on the c-Src-Caspase-8 interaction (Fig 4C). In untreated A549 and H522 cells, Caspase-8 and RIPK1 didnot coimmunoprecipitate with FADD, which was accompanied by frequent binding of c-FLIP to FADD (Figs 4D and S4C). Caspase-8 binding to FADD resulted in remarkably decreased c-FLIP binding to trigger apoptotic cell death in the paclitaxel-treated A549 cellstransduced with c-Src shRNA (Figs 4D and 4C), whereas p-Casp8was not bound to FADD in the paclitaxel-treated A549 and H522 cells(Figs 4D and S4C). RIPK1 was significantly increased in the coimmunoprecipitated complex with an antibody specific for FADD in the paclitaxel-treated A549 and H522 cells with deficient or phosphorylated Caspase-8 (Figs 4D and S4C). We next determined how FADD affected paclitaxel-induced cell death. FADD silencingvia lentiviral delivery of shRNA (Figs S4D and S4E) was able to rescue A549 and H522 cells from paclitaxel-induced apoptosis or necroptosis (Figs 4E and S4F). FADD silencing proficiently inhibited the phosphorylation of RIPK1, RIPK3 and MLKL in A549 cells transduced with control or Caspase-8 shRNA (Fig 4F) and the apoptotic cleavage of Caspase-8 in A549 cells transduced with c-Src shRNA (Fig S4G). Similarly, FADD knockdown ablated RIPK1/RIPK3/MLKL activation to block the necroptosis of H522 cells (Fig 4G). The antitumor activity of FADD in the paclitaxel-induced cell death was confirmed by *in vivo* xenograft analysis (Figs S4H and S4I). Taken

together, itsuggestedthat FADD promoted thepaclitaxel-inducedcell deathof lung adenocarcinomaviathe assembly of FADD-c-FLIP-Caspase-8-RIPK1.

To elucidate the role of c-FLIP in paclitaxel-induced cell death, c-FLIP in A549 cells was knocked downwith lentiviral shRNA (Fig S4J). Surprisingly, c-FLIP knockdown did not alterthe apoptosis and necroptosis in A549 cells (Figs S4J and S4K). In the immunoprecipitated complex using FADD antibodyin paclitaxel-treated A549 cells, c-FLIP knockdown did not affect the interaction between RIPK1/Caspase-8 and FADD (Fig S4L). Consistently, c-FLIP knockdown did not affect the paclitaxel-induced H522 cell death (Figs S4M and S4N),while the interaction between FADD and RIPK1/Caspase-8 was notaffected by c-FLIP in H522 cells (Fig S4O). These data indicated that c-FLIP might suppress apoptosis in untreated cells and doesnot affect cell death under paclitaxel treatment.

lncRNA-related chemotherapy resistance in lung adenocarcinoma (lncCRLA) inhibited RIPK1-induced necroptosis inthe mesenchymal-like lung adenocarcinoma.

Necroptosis was obviously attenuated in themesenchymal-like lung adenocarcinoma cells under paclitaxel treatment compared with that in theepithelial-likelung adenocarcinoma cells. We explored whether EMT contributed to resistance to paclitaxel in lung adenocarcinoma. An antibody againstβ-catenin, 7A7, was delivered to blockβ-catenin nuclear translocation, which inhibits EMT withnoeffects on the c-Src-Caspase-8 interaction [14]. 7A7 antibody delivery promotednecroptotic cell death with RIPK1/RIPK3/MLKL activation in A549 and H522 cells and had no effect on c-Src-induced Caspase-8 phosphorylation (Figs 5A 5B and S5A). The transfection of constitutively active c-Src (Src Y527F)into Caspase-8-deficientH522 cellspromoted EMT[17]and reduced RIPK1-induced necroptosis (Fig S4A). This finding suggested that EMT in lung adenocarcinoma obviously reduced paclitaxel-triggered necroptotic cell deathin lung adenocarcinoma.

Mounting evidence has indicated that lncRNAsarecritical for chemotherapy resistance in various human tumors [23, 24]. In an attempt to identify the lncRNA(s) required for EMT-related resistance to paclitaxelin mesenchymal-like lung adenocarcinoma cells, we conducted two sequential rounds of screening (Fig S5B). First, a lncRNA microarray was utilized to compare lncRNA expression profiles between the mesenchymal-like (A549+Control-Mesenchymal) and the epithelial-like (A549+Caspase-8/c-Src shRNA-Epithelial) A549 cells (Fig 5C). The 8 most differentially expressed lncRNAs (fold change >8-fold, Figs5D S5C and TableS3)were validated by qRT-PCR in A549 cells and H522 cells (Figs 5E and S5C). Then, selected lncRNAs were subjected to loss-of-function and gain-of-function analyses in the mesenchymal-like and the epithelial-like cells, respectively (Figs S5D and S5F). In the mesenchymal-like A549 cells (A549+Control), of the8 most differentially expressed lncRNAs, lncRNA 444464 was the only one to increase the sensitivity to paclitaxel when knocked down (Figs 5F and 5G). Notably, lncRNA 444464 failed to rescue paclitaxel-induced death of A549+c-Src shRNA cells (Fig S5E), but was able to obviously decrease paclitaxel-induced death of A549+Caspase-8 shRNA cells (Fig S5G). Therefore, we focused on the uncharacterized lncRNA 444464 (*ENST00000444464*) and named it lncRNA-related chemotherapy resistance in lung adenocarcinoma (lncCRLA). This long-coding RNA was located on chromosome 17 in

humans and 512 ntin length (Fig S5H). The noncoding nature of lncCRLA was confirmed by coding potential analysis (Fig S5I). Consistently, the mesenchymal-like H522 cells(H522+Src Y527F/Caspase-8-Mesenchymal) had a much higher level of lncCRLA than the epithelial-like H522 cells (H522+Control-Epithelial, Fig S5J), and transduction of lncCRLA shRNA efficiently enhanced cell death (Fig 5H).We transfectedexogenous lncCRLA into H522 cells, which led to a reduction in cell death (Fig S5K). Todissect the functional role of lncCRLA, we stably overexpressed lncCRLA in Caspase-8-lacking epithelial-like cells viaadenoviral transduction and stably knocked downlncCRLA in the p-Casp8-positive mesenchymal-like cells via lentiviral shRNA. lncCRLAblocked RIPK1-induced necroptotic signaling and reduced the number of PI-positive cellsin mesenchymal-like A549 and H522 cells (Fig 5I). In the epithelial-like tumor cells, lncCRLA conferred resistance to paclitaxel-induced necroptosis (Fig S5L). Taken together, these data indicated that lncCRLA efficiently hampered paclitaxel-induced necroptotic cell death,butdid not affect paclitaxel-induced apoptotic cell death in lung adenocarcinoma.

We sought to determine how lncCRLA influenced paclitaxel-induced necroptosis. It revealed that lncCRLAwas predominantly located in the cytoplasm of A549+Control cells (Fig S5M). lncCRLA might function as a competing endogenous RNA to sequester microRNAs (miRNAs)leading to the liberation of corresponding miRNA-targeted transcripts. Subsequent bioinformatics analysis by TargetScan and miRandashowedno putative miRNA response elements. How didlncCRLA impair paclitaxel-mediated RIPK1-induced necroptosis? The radioimmunoprecipitation (RIP) assay showed that lncCRLA interacts with RIPK1 but not RIPK3 in paclitaxel-treated mesenchymal-like tumor cells(Figs 5J and S5N). The RNA pull-down assay confirmed the interaction between RIPK1 and lncCRLA in H522 cells with ectopic lncCRLAexpression (Fig S5O). To validate the target domain of RIPK1 for lncCRLA, truncated RIPK1 constructs were created with HA tag (Fig S5P) and stably transfected into the lncCRLA-expressing H522 cells with RIPK1 knockdown viaadenoviral shRNA. The functional role of lncCRLA was determined by its binding to the intermediate domain (ID) of RIPK1 independent of the kinase domain (KD) and DD (Fig S5P). It was reasonable that binding of RIPK1 to lncCRLAblockedthe RHIM of RIPK1, leading to the inability of RIPK3 to interactwith the RHIM of RIPK1 to elicit resistance to paclitaxel in lung adenocarcinoma.

We investigated how lncCRLA was upregulated in the mesenchymal-like lung adenocarcinoma cells. Our previous study revealed that the transcriptional activity of transcription factor 4 (TCF-4) was predominant in inducing the EMT phenotype in lung adenocarcinoma [17]. We hypothesized that TCF-4 functioned as a transcription factor to upregulate lncCRLA. Afterthe promoter region of lncCRLA was reviewed, two Wnt-responsive elements (WRE) were detected between –286 and -292 (5’-CTTTGTG-3’) and between –96 and -102 of the transcription start site (TSS) (5’-CTTTGGC-3’). We constructed a set of lncCRLApromoters linked to a luciferase reporter in the mesenchymal-like tumor cells. As shown in Figure 5K, the lncCRLApromoter was able to markedly increase the luciferase activity in the mesenchymal-like lung adenocarcinoma cells, which was confirmed by ChIP assay using an antibody specific for TCF-4(Fig S5Q).

We next investigatedlncCRLAexpression and the relationship between lncCRLA and chemotherapy response in patients with lung adenocarcinoma. lncCRLAexpression was determined by locked nucleic acid (LNA)-based in situ hybridization (ISH) (Fig 5L) and was significantly increased in patients with resectable and metastatic lung adenocarcinoma who had progressive disease (PD)(Figs 5M and S5R). Moreover, lncCRLA expression was positively correlated with p-Casp8 expression (Fig S5S). Low levels of lncCRLA produced a marked benefit for PFS in the patients with resectable lung adenocarcinoma (Fig S5T). Taken together, these data suggested that upregulation oflncCRLA enhanced chemotherapy resistanceofthe mesenchymal-like lung adenocarcinomato paclitaxel by directly binding to RIPK1 to block necroptosis.

c-Src inhibitor,dasatinib and c-FLIP knockdown sensitized the mesenchymal-like lung adenocarcinoma cells to paclitaxel-induced cytotoxicity.

The prior resultsindicated that c-Src overactivation viaits interaction with phosphorylated Caspase-8 triggered EMT to yield a limited benefit for paclitaxel treatment[17]. Hence, we determined whether the c-Src inhibitor dasatinib could increase the therapeutic benefit of paclitaxel through EMT blockade and Caspase-8 dephosphorylation. Dasatinib was capable of ablating the effects of Caspase-8 phosphorylation and c-Src activation in A549+Control and H522+Caspase-8 (Fig 6A), in whichdasatinib efficiently blocked the EMT phenotype and lncCRLA expression (Figs S6A, S6B and S6C). Dasatinib sensitized lung adenocarcinoma cells to paclitaxel (Fig 6B). Surprisingly, the proportion of PI-positive cells increased by approximately 30% in cells treated with paclitaxel plus dasatinib (Fig 6C), while theproportion of Annexin V-positive cells was comparable among thevarious cell lines (Fig 6C). The contribution of dasatinib to the therapeutic efficacy of paclitaxel in lung adenocarcinoma was confirmedby an *in vivo* xenograft experiment (Figs 6D and 6E). Consistently, dasatinib enhanced necroptosis by activating RIPK1/RIPK3/MLKL but did not enhance the apoptotic cleavage of Caspase-8 in the mesenchymal-like A549 and H522 cells when combined with paclitaxel (Fig 6F).

Subsequently, we investigated why Caspase-8 dephosphorylation viadasatinib-induced c-Src inactivation did notlead to apoptotic cell death. It was noteworthy thatin the paclitaxel-treated A549 and H522 cells, dephosphorylated Caspase-8 induced by dasatinibdidnot coimmunoprecipitate with FADD, while c-FLIP, an inhibitor ofCaspase-8-induced apoptosis, predominantly bound to FADD independent of dasatinibaddition (Fig S6D). The interaction between RIPK1 and FADD was strengthened by the addition of dasatinib (Fig S6D). It was more likely that blockingphosphorylated Caspase-8 from binding FADD accounted for the mechanism by which dasatinib-mediated dephosphorylated Caspase-8 could not bind FADD due to c-FLIP occupying the binding pocket.

To explore the influence of c-FLIP on the sensitivity of lung adenocarcinoma to paclitaxel and dasatinib, we constructed 5 siRNAs targeting c-FLIP. According to knockdown efficiency of the siRNAs in A549+Control and H522+Caspase-8 (Figs S6E and S6F), we selected siRNA2 and siRNA4 to construct lentiviral shRNA1 and shRNA2 stably transfected into tumor cells. c-FLIP knockdown markedly promoted the apoptosis of A549 and H522 cells treated with dasatinibplus paclitaxel (Figs 6G, S6G and S6H). c-

FLIP knockdown did not affect RIPK1 activation, but Caspase-8 was recruited to FADD and apoptoticallycleaved in both cell lines, in which shRNA1 and shRNA2 of c-FLIP yielded similar effects with different knockdown level of c-FLIP (Figs S6I and S6J). Intriguingly, both c-FLIP shRNA1 and shRNA2 similarly facilitated apoptosis in the A549+c-Src shRNA treated with paclitaxel (Figs S6K and S6L). c-FLIP knockdown by shRNA2 suppressed tumor growth in A549 cells with control shRNA and H522 cells with Caspase-8 in*in vivo* xenograft experiments (Fig 6H). We observed that c-FLIP shRNA2 did not restrict the therapeutic benefit with a lesser attenuation in c-FLIP expression compared with c-FLIP shRNA1, suggesting that a reduction in c-FLIP expression to some extent was sufficient to sensitize the paclitaxel+dasatinib treatment in lung adenocarcinoma.

Accordingly, we tested the possibility of delivering siRNA targeting c-FLIP combined with paclitaxel liposomes. The paclitaxel liposome plus c-FLIP siRNA (siFLIP) was constructed on the basis of paclitaxel liposomes as a common pharmacologicaldelivery mechanism (Fig 6I). As shown in Figure S6M, paclitaxel liposomes had a great potential to transducesiFLIP into A549 cells. Paclitaxel liposome+siFLIPreduced the mRNA and protein levels of c-FLIP in the mesenchymal-like A549+Control and H522+Caspase-8 cells (Figs 6J and S6N), while paclitaxel liposome+siFLIPcombined with dasatinib predominantly eliminated tumor cells *in vivo* and *in vitro* (Figs S6O and S6P). Then, we established a patient-derived xenograft (PDX) model to determine the response of lung adenocarcinoma to the combination of paclitaxel liposome+siFLIP and dasatinib. To adequately utilize the patient-derived sample, a PDX model was designed and illustrated in Figure S6Q, and patients involved in the PDX experiment were listed in Table S4. Accordingly, paclitaxel liposome+siFLIP plus dasatinib was significantly superior ininhibiting the growth of tumorcellsfrom patients with resectable lung adenocarcinoma compared with other treatments (Figs 6K and S6R). Collectively, c-FLIP knockdown was able to sensitize the mesenchymal-like lung adenocarcinoma to dual therapies of paclitaxel plus dasatinib.

Discussion

During the process ofbecoming more invasive and motile, cancer cells that have undergone EMT also acquire resistance to several drugs and chemotherapeutic agents [6]. Our prior work showed that the c-Src-Caspase-8 interaction was able to specifically phosphorylate Caspase-8 at tyrosine 380 and overactivate c-Src tofacilitate EMT [16]. We generalized our notion that EMT occurred when c-Src-mediated phosphorylation ofCaspase-8 overactivated c-Src in a positive feedback loop. It was of major interest that Caspase-8 phosphorylation wasascribed to c-Src expression level in lung adenocarcinoma. Although c-Srcisactivated by multiple growth and metastatic signaling pathways[25], we determinedthat phosphorylated Caspase-8 by c-Src played a key role inoveractivating c-Src to trigger EMT in lung adenocarcinoma. Our team has focused heavilyon the basic activation of c-Srcprior toCaspase-8 phosphorylation (data unpublished).Multiple EMTfactors and EMTsignaling are more pronounced in cancer tissues[26, 27]. Although a plethora of biomarkers have been utilized in the EMT process, Vim and E-cad are likely the best markers in lung adenocarcinoma [15]. We found that p-Casp8-expressing lung adenocarcinoma tissues had the propensity to present with a mesenchymal phenotype with

downregulated E-cad and upregulated Vim and corresponded toa lower response rate to treatment and a worse 5-year PFS. It was rationalized that p-Casp8 was responsible for disease progression arising from the EMT phenotype and chemoresistance in patients with lung adenocarcinoma.

Combined paclitaxel and cisplatin has been thecornerstone for NSCLC treatment for many years;both drugs have completely different mechanismsin eliminating cancer cells[28]. p53 plays a central role in cisplatin-induced cell death [29]. Consistently, our results unveiled that cisplatin killedlung adenocarcinoma cells independent of Caspase-8 and c-Src. In parallel, paclitaxel increased mitotic arrest regardless of Caspase-8 or c-Src as well as markedly induced cell death in aCaspase-8-dependent manner. Thus, we sought to determine whether p-Casp8 might be the lynchpin for EMT-related chemoresistance.

Necroptosis was observed to be a compensatory mechanism under the condition of apoptotic blockade [30, 31]. We detected that phosphorylatingCaspase-8 by c-Src or silencing Caspase-8 rescued numerous lung adenocarcinoma cells from cell death but failed to prevent 10-30% necroptoticcell death from paclitaxel. These results implied that Caspase-8 phosphorylation or silencing yielded resistance to paclitaxel due to apoptotic inhibition. Traditionally, paclitaxel, an antimitotic drug, disrupts spindle assembly leading to mitotic arrest by persistent activation of the spindle assembly checkpoint (SAC). Following prolonged arrest, cells either die in mitosis or undergo “slippage,” returning to interphase without completing cell division [32, 33]. More recently, mitotic arrest was reported to lead to DNA damage and genetic instability, which doesnot give rise to a large number of cell deaths [34, 35]. Our results showed that paclitaxel increased the proportion of cells inmitotic arrest independently of Caspase-8 corresponding to a disproportionately increasedamount of cell death dependently of Caspase-8. Therefore, paclitaxel-induced mitoticarrest can be distinguished from its tumoricidal function.

FADD, Caspase-8 and c-FLIP inhibited necroptosis by suppressing RIPK1 and RIPK3 within this complex [36],while FADD-Caspase-8-c-FLIPcomplex inhibition resulted in the FADD-induced assembly of RIPK1–RIPK3 complex for necroptosis [37, 38]. The assembly of RIPK1-RIPK3 complex via RHIM in response toa variety of stimuli was critical to initiate RIPK1 phosphorylation, which was required for RIPK3-RIPK3 dimerization and RIPK3 phosphorylation, eventually resulting in MLKL phosphorylation to trigger necroptosis [39, 40].It was approved by our observation that FADD was required to recruit RIPK1 leading to necroptosis and Caspase-8 to induce apoptosis following paclitaxel treatment.These results indicated that FADD functioned as a sensor for cell death stimuli under paclitaxel treatment.

FADD-c-FLIP complex in the absence ofCaspase-8 and RIPK1 existedunder no treatment. Under paclitaxel stimulation, Caspase-8 replaced c-FLIP and interacted withFADD-involved complex to trigger apoptosis in lung adenocarcinoma cells with unphosphorylated Caspase-8.It was hypothesized that Caspase-8 possesses ahigher affinity to FADD relative to c-FLIP under apoptotic stimuli.Caspase-8-c-FLIP based on FADD was reported to inhibit necroptosis by cleaving RIPK1 (at D324) and RIPK3 (at D333) within this complex[37]. Nevertheless, RIPK1 and RIPK3 showedsimilar expression levelsbefore and after paclitaxel treatment. We found that RIPK1-induced necroptosis was undetectable with the onset of apoptosis in the

paclitaxel-treated A549 cells with c-Src shRNA. It was postulated that apoptosis still counteracted RIPK1-induced necroptosis by restricting RIPK1 involvement instead of cleaving RIPK1. It was intriguing thatknockdown of c-FLIP did not enhanceA549 and H522 cell deathwith paclitaxel treatment.This was attributed to two mechanisms:c-FLIP was replaced by Caspase-8 under apoptotic conditions, while c-FLIP had no influence on necroptosis under necroptotic conditions.

Although Caspase-8 phosphorylation and Caspase-8 deficiency impaired apoptosis under paclitaxel treatment, Caspase-8 phosphorylation induced a smaller amountof necroptotic death than did Caspase-8 deficiency.Caspase-8 phosphorylation by c-Src initiated EMT to protect tumor cells from paclitaxel-induced antitumor activity. This notion wassupportedby the observation that compared with the mesenchymal-like A549 cells with control shRNA, the epithelial-like A549 cells with RNF43 shRNA presenting c-Src-Caspase-8 interaction had a higher proportion of cells killed viapaclitaxel-induced necroptosis. We focused onthe contribution oflncRNAsto the resistanceof lung adenocarcinoma to paclitaxel. After lncRNA microarray profiling, lncCRLAhad the most outstanding effects on the resistance to paclitaxel in the mesenchymal-like lung adenocarcinoma bybinding to the ID of RIPK1 to interfere withRIPK1-RIPK3 interaction-based necroptosis. The RHIM domain in the ID of RIPK1 was blockedto hamper itsinteraction with RIKP3. In addition, exogenous lncCRLA expression rescued the Caspase-8-deficientepithelial-like lung adenocarcinoma from necroptosis.

Dasatinibhas beencharacterized as one of the most efficient antagonists for c-Src and has been recently approved for clinical use inacute lymphoblastic leukemia and several solid tumors [41, 42]. Dasatinib did not increase apoptotic cell death through Caspase-8 cleavage but increased necroptosis in lung adenocarcinoma. Mechanistically, FADD was excessively occupied by c-FLIP in cells withCaspase-8 phosphorylation, butphosphorylated Caspase-8 was dissociated fromFADD under paclitaxel treatment. Therefore, Caspase-8 dephosphorylation could not trigger apoptotic cleavage due to dephosphorylated Caspase-8 dissociated from FADD. On the other hand, dasatinib facilitated necroptosis by blocking EMTandsuppressinglncCRLA expression. We expected the activation ofapoptosis and necroptosis to significantly increase antitumor effects in the mesenchymal-like lung adenocarcinoma with p-Casp8. Our team collaboratedwith the LvYe pharmacy to create paclitaxel liposomes encapsulating siFLIP, which had been verified to function as a strong antitumor agent and combined these liposomes with dasatinibto treat themesenchymal-like lung adenocarcinoma. It was noteworthy that c-FLIP knockdown to a lesser extent was sufficient to initiate apoptotic function of Caspase-8.

Conclusions

c-Src-mediated Caspase-8 phosphorylation, which isessential for the EMT phenotype through c-Src overactivation in lung adenocarcinoma cell lines.The shift of these cells to the mesenchymal phenotypeleadsto chemoresistance tocisplatin plus paclitaxel in patients with resectable lung adenocarcinoma,who also have a significantly worse 5-yearPFS rate. Cisplatin killedlung adenocarcinoma cells independent of Caspase-8 status, while paclitaxel triggered necroptosis in lung adenocarcinoma cells with Caspase-8 phosphorylation or deficiency, during which FADD interactedwith

RIPK1 via the DD to blockRIPK1/RIPK3/MLKL signaling. Furthermore, a brand-new lncRNA, named lncCRLA, was significantly upregulated by TCF-4 andinhibited RIPK1-induced necroptosis in the mesenchymal-like lung adenocarcinoma cellsby impairingof RIPK1-RIPK3 interaction via binding to the ID of RIPK1. Dasatinib enhanced necroptosis in paclitaxel-treated lung adenocarcinoma cells that underwentEMT, while c-FLIP knockdown predominantly sensitized mesenchymal-like lung adenocarcinoma to dasatinib+paclitaxel throughapoptosis.Together, the c-Src-Caspase-8 interaction initiated the EMT phenotype and chemoresistance by Caspase-8 phosphorylation and chemoresistance-related lncRNA expression, to which treatment with dasatinib plus paclitaxel liposome + siFLIP was lethal (Fig 7).

List Of Abbreviations:

Non-small cell lung cancer (NSCLC); Epithelial-mesenchymal transition (EMT); Fas-associated protein with death domain (FADD); cellular FLICE (FADD-like IL-1β-converting enzyme)-inhibitory protein (long) (c-FLIP); Receptor-interacting serine/threonine-protein kinase 1/3 (RIPK1/3); RIP homotypic interaction motif (RHIM); Mixed lineage kinase domain-like (MLKL); Necrostatin-1 (nec-1); E-cadherin (E-cad); Vimentin (Vim); Phosphorylated Caspase-8 at the tyrosine 380 (p-Casp8); Activated c-Src at the tyrosine 527 (p-Src); Complete response (CR); Partial response (PR); Spindle assembly checkpoint (SAC); Death effector domain (DED); Death domain (DD); Intermediate domain (ID); Kinase domain (KD); Transcription factor 4 (TCF-4); Locked nucleic acid (LNA)-based in situ hybridization (ISH); Chemotherapy resistance in lung adenocarcinoma (lncCRLA); c-FLIP siRNA (siFLIP); tumor growth factor-β (TGF-β); Patient-derived xenograft (PDX); National Cancer Institute (NCI); American Type Culture Collection (ATCC); American Joint Committee on Cancer (AJCC); immunohistochemistry (IHC); fetal bovine serum (FBS); short hairpin RNAs (shRNAs); hemagglutinin (HA); RNA immunoprecipitation assay (RIP assay); Chromatin immunoprecipitation assay(ChIP assay); Propidium iodide (PI).

Declarations

Ethics approval and consent to participate

The procedures of this study, including 7 references, were approved by the Ethics Committee of the Second Affiliated Hospital of Xi'an Jiaotong University.The experiments were performedupon receiving written consent from each subject.The study methodologies conformed to the standards set by the Declaration of Helsinki.

Consent for publication

All authors approved for paper publication.

Availability of data and materials

All data and materials were available when required.

Competing interests

No

Funding

Supported by National Natural Science Foundation of China (No. 81301847 and No. 81872390)

Authors' contributions

Conceptionanddesign: Yang Zhao

Administrativesupport:Shuqun Zhang, Weili Min

Provisionofstudymaterialsorpatients: Yang Zhao, Liangzhang Sun, Xiao Gao, Xiao Gao, Weili Min

Collectionandassemblyofdata: Yang Zhao, Liangzhang Sun, Xiao Gao

Manuscriptwriting: Yang Zhao

Finalapprovalofmanuscript: Yang Zhao

Acknowledgements

No

References:

1. [1] R.L. Siegel, K.D. Miller, A. Jemal, Cancer statistics, 2018, CA Cancer J Clin, 68 (2018) 7-30.
2. [2] R. Zheng, H. Zeng, T. Zuo, S. Zhang, Y. Qiao, Q. Zhou, W. Chen, Lung cancer incidence and mortality in China, 2011, Thorac Cancer, 7 (2016) 94-99.
3. [3] G.R. Oxnard, A. Binder, P.A. Janne, New targetable oncogenes in non-small-cell lung cancer, J Clin Oncol, 31 (2013) 1097-1104.
4. [4] M. Jamal-Hanjani, G.A. Wilson, N. McGranahan, N.J. Birkbak, T.B.K. Watkins, S. Veeriah, S. Shafi, D.H. Johnson, R. Mitter, R. Rosenthal, M. Salm, S. Horswell, M. Escudero, N. Matthews, A. Rowan, T. Chambers, D.A. Moore, S. Turajlic, H. Xu, S.M. Lee, M.D. Forster, T. Ahmad, C.T. Hiley, C. Abbosh, M. Falzon, E. Borg, T. Marafioti, D. Lawrence, M. Hayward, S. Kolvekar, N. Panagiotopoulos, S.M. Janes, R. Thakrar, A. Ahmed, F. Blackhall, Y. Summers, R. Shah, L. Joseph, A.M. Quinn, P.A. Crosbie, B. Naidu, G. Middleton, G. Langman, S. Trotter, M. Nicolson, H. Remmen, K. Kerr, M. Chetty, L. Gomersall, D.A. Fennell, A. Nakas, S. Rathinam, G. Anand, S. Khan, P. Russell, V. Ezhil, B. Ismail, M. Irvin-Sellers, V. Prakash, J.F. Lester, M. Kornaszewska, R. Attanoos, H. Adams, H. Davies, S. Dentro, P. Taniere, B. O'Sullivan, H.L. Lowe, J.A. Hartley, N. Iles, H. Bell, Y. Ngai, J.A. Shaw, J. Herrero, Z. Szallasi, R.F. Schwarz, A. Stewart, S.A. Quezada, J. Le Quesne, P. Van Loo, C. Dive, A. Hackshaw, C. Swanton, T.R.

Consortium, Tracking the Evolution of Non-Small-Cell Lung Cancer, N Engl J Med, 376 (2017) 2109-2121.

5. [5] R.S. Herbst, D. Morgensztern, C. Boshoff, The biology and management of non-small cell lung cancer, Nature, 553 (2018) 446-454.
6. [6] K.R. Fischer, A. Durrans, S. Lee, J. Sheng, F. Li, S.T. Wong, H. Choi, T. El Rayes, S. Ryu, J. Troeger, R.F. Schwabe, L.T. Vahdat, N.K. Altorki, V. Mittal, D. Gao, Epithelial-to-mesenchymal transition is not required for lung metastasis but contributes to chemoresistance, Nature, 527 (2015) 472-476.
7. [7] A. Chang, Chemotherapy, chemoresistance and the changing treatment landscape for NSCLC, Lung Cancer, 71 (2011) 3-10.
8. [8] T. Brabletz, EMT and MET in metastasis: where are the cancer stem cells?, Cancer Cell, 22 (2012) 699-701.
9. [9] J.P. Thiery, C.T. Lim, Tumor dissemination: an EMT affair, Cancer Cell, 23 (2013) 272-273.
10. [10] J.H. Tsai, J.L. Donaher, D.A. Murphy, S. Chau, J. Yang, Spatiotemporal regulation of epithelial-mesenchymal transition is essential for squamous cell carcinoma metastasis, Cancer Cell, 22 (2012) 725-736.
11. [11] R. Kalluri, R.A. Weinberg, The basics of epithelial-mesenchymal transition, J Clin Invest, 119 (2009) 1420-1428.
12. [12] S. Seton-Rogers, Epithelial-mesenchymal transition: Untangling EMT's functions, Nat Rev Cancer, 16 (2016) 1.
13. [13] X. Zheng, J.L. Carstens, J. Kim, M. Scheible, J. Kaye, H. Sugimoto, C.C. Wu, V.S. LeBleu, R. Kalluri, Epithelial-to-mesenchymal transition is dispensable for metastasis but induces chemoresistance in pancreatic cancer, Nature, (2015).
14. [14] Y. Diao, X. Ma, W. Min, S. Lin, H. Kang, Z. Dai, X. Wang, Y. Zhao, Dasatinib promotes paclitaxel-induced necroptosis in lung adenocarcinoma with phosphorylated caspase-8 by c-Src, Cancer Lett, 379 (2016) 12-23.
15. [15] M.J. Schliekelman, A. Taguchi, J. Zhu, X. Dai, J. Rodriguez, M. Celiktas, Q. Zhang, A. Chin, C.H. Wong, H. Wang, L. McFerrin, S.A. Selamat, C. Yang, E.M. Kroh, K.S. Garg, C. Behrens, A.F. Gazdar, I.A. Laird-Offringa, M. Tewari, Wistuba, II, J.P. Thiery, S.M. Hanash, Molecular portraits of epithelial, mesenchymal, and hybrid States in lung adenocarcinoma and their relevance to survival, Cancer Res, 75 (2015) 1789-1800.
16. [16] S. Cursi, A. Rufini, V. Stagni, I. Condo, V. Matafora, A. Bachi, A.P. Bonifazi, L. Coppola, G. Superti-Furga, R. Testi, D. Barila, Src kinase phosphorylates Caspase-8 on Tyr380: a novel mechanism of apoptosis suppression, EMBO J, 25 (2006) 1895-1905.
17. [17] Y. Zhang, L. Sun, X. Gao, A. Guo, Y. Diao, Y. Zhao, RNF43 ubiquitinates and degrades phosphorylated E-cadherin by c-Src to facilitate epithelial-mesenchymal transition in lung adenocarcinoma, BMC Cancer, 19 (2019) 670.
18. [18] W. Wei, M.J. Birrer, Spleen Tyrosine Kinase Confers Paclitaxel Resistance in Ovarian Cancer, Cancer Cell, 28 (2015) 7-9.

19. [19] A. Linkermann, D.R. Green, Necroptosis, N Engl J Med, 370 (2014) 455-465.
20. [20] L. Wang, F. Du, X. Wang, TNF-alpha induces two distinct caspase-8 activation pathways, Cell, 133 (2008) 693-703.
21. [21] Y. Yu, S. Gaillard, J.M. Phillip, T.C. Huang, S.M. Pinto, N.G. Tessarollo, Z. Zhang, A. Pandey, D. Wirtz, A. Ayhan, B. Davidson, T.L. Wang, M. Shih Ie, Inhibition of Spleen Tyrosine Kinase Potentiates Paclitaxel-Induced Cytotoxicity in Ovarian Cancer Cells by Stabilizing Microtubules, Cancer Cell, 28 (2015) 82-96.
22. [22] Y. Boege, M. Malehmir, M.E. Healy, K. Bettermann, A. Lorentzen, M. Vucur, A.K. Ahuja, F. Bohm, J.C. Mertens, Y. Shimizu, L. Frick, C. Remouchamps, K. Mutreja, T. Kahne, D. Sundaravinayagam, M.J. Wolf, H. Rehrauer, C. Koppe, T. Speicher, S. Padrissa-Altes, R. Maire, J.M. Schattenberg, J.S. Jeong, L. Liu, S. Zwirner, R. Boger, N. Huser, R.J. Davis, B. Mullhaupt, H. Moch, H. Schulze-Bergkamen, P.A. Clavien, S. Werner, L. Borsig, S.A. Luther, P.J. Jost, R. Weinlich, K. Unger, A. Behrens, L. Hillert, C. Dillon, M. Di Virgilio, D. Wallach, E. Dejardin, L. Zender, M. Naumann, H. Walczak, D.R. Green, M. Lopes, I. Lavrik, T. Luedde, M. Heikenwalder, A. Weber, A Dual Role of Caspase-8 in Triggering and Sensing Proliferation-Associated DNA Damage, a Key Determinant of Liver Cancer Development, Cancer Cell, 32 (2017) 342-359 e310.
23. [23] L. Qu, J. Ding, C. Chen, Z.J. Wu, B. Liu, Y. Gao, W. Chen, F. Liu, W. Sun, X.F. Li, X. Wang, Y. Wang, Z.Y. Xu, L. Gao, Q. Yang, B. Xu, Y.M. Li, Z.Y. Fang, Z.P. Xu, Y. Bao, D.S. Wu, X. Miao, H.Y. Sun, Y.H. Sun, H.Y. Wang, L.H. Wang, Exosome-Transmitted lncARSR Promotes Sunitinib Resistance in Renal Cancer by Acting as a Competing Endogenous RNA, Cancer Cell, 29 (2016) 653-668.
24. [24] X. Yan, Z. Hu, Y. Feng, X. Hu, J. Yuan, S.D. Zhao, Y. Zhang, L. Yang, W. Shan, Q. He, L. Fan, L.E. Kandalaft, J.L. Tanyi, C. Li, C.X. Yuan, D. Zhang, H. Yuan, K. Hua, Y. Lu, D. Katsaros, Q. Huang, K. Montone, Y. Fan, G. Coukos, J. Boyd, A.K. Sood, T. Rebbeck, G.B. Mills, C.V. Dang, L. Zhang, Comprehensive Genomic Characterization of Long Non-coding RNAs across Human Cancers, Cancer Cell, 28 (2015) 529-540.
25. [25] S. Boumahdi, F.J. de Sauvage, The great escape: tumour cell plasticity in resistance to targeted therapy, Nat Rev Drug Discov, (2019).
26. [26] W. Lu, Y. Kang, Epithelial-Mesenchymal Plasticity in Cancer Progression and Metastasis, Dev Cell, 49 (2019) 361-374.
27. [27] N.M. Aiello, Y. Kang, Context-dependent EMT programs in cancer metastasis, J Exp Med, 216 (2019) 1016-1026.
28. [28] M. Di Maio, P. Chiodini, V. Georgoulias, D. Hatzidaki, K. Takeda, F.M. Wachters, V. Gebbia, E.F. Smit, A. Morabito, C. Gallo, F. Perrone, C. Gridelli, Meta-analysis of single-agent chemotherapy compared with combination chemotherapy as second-line treatment of advanced non-small-cell lung cancer, J Clin Oncol, 27 (2009) 1836-1843.
29. [29] L. Galluzzi, I. Vitale, J. Michels, C. Brenner, G. Szabadkai, A. Harel-Bellan, M. Castedo, G. Kroemer, Systems biology of cisplatin resistance: past, present and future, Cell Death Dis, 5 (2014) e1257.

30. [30] L. Galluzzi, G. Kroemer, Necroptosis: a specialized pathway of programmed necrosis, Cell, 135 (2008) 1161-1163.
31. [31] W. Zhou, J. Yuan, SnapShot: Necroptosis, Cell, 158 (2014) 464-464 e461.
32. [32] F. Gulluni, M. Martini, M.C. De Santis, C.C. Campa, A. Ghigo, J.P. Margaria, E. Ciraolo, I. Franco, U. Ala, L. Annaratone, D. Disalvatore, G. Bertalot, G. Viale, A. Noatynska, M. Compagno, S. Sigismund, F. Montemurro, M. Thelen, F. Fan, P. Meraldi, C. Marchio, S. Pece, A. Sapino, R. Chiarle, P.P. Di Fiore, E. Hirsch, Mitotic Spindle Assembly and Genomic Stability in Breast Cancer Require PI3K-C2alpha Scaffolding Function, Cancer Cell, 32 (2017) 444-459 e447.
33. [33] C. Topham, A. Tighe, P. Ly, A. Bennett, O. Sloss, L. Nelson, R.A. Ridgway, D. Huels, S. Littler, C. Schandl, Y. Sun, B. Bechi, D.J. Procter, O.J. Sansom, D.W. Cleveland, S.S. Taylor, MYC Is a Major Determinant of Mitotic Cell Fate, Cancer Cell, 28 (2015) 129-140.
34. [34] S.M. Harding, J.L. Benci, J. Irianto, D.E. Discher, A.J. Minn, R.A. Greenberg, Mitotic progression following DNA damage enables pattern recognition within micronuclei, Nature, (2017).
35. [35] M. Macheret, T.D. Halazonetis, DNA replication stress as a hallmark of cancer, Annu Rev Pathol, 10 (2015) 425-448.
36. [36] M. Dannappel, K. Vlantis, S. Kumari, A. Polykratis, C. Kim, L. Wachsmuth, C. Eftychi, J. Lin, T. Corona, N. Hermance, M. Zelic, P. Kirsch, M. Basic, A. Bleich, M. Kelliher, M. Pasparakis, RIPK1 maintains epithelial homeostasis by inhibiting apoptosis and necroptosis, Nature, 513 (2014) 90-94.
37. [37] D. Moquin, F.K. Chan, The molecular regulation of programmed necrotic cell injury, Trends Biochem Sci, 35 (2010) 434-441.
38. [38] A. Oberst, D.R. Green, It cuts both ways: reconciling the dual roles of caspase 8 in cell death and survival, Nat Rev Mol Cell Biol, 12 (2011) 757-763.
39. [39] J.A. Rickard, J.A. O'Donnell, J.M. Evans, N. Lalaoui, A.R. Poh, T. Rogers, J.E. Vince, K.E. Lawlor, R.L. Ninnis, H. Anderton, C. Hall, S.K. Spall, T.J. Phesse, H.E. Abud, L.H. Cengia, J. Corbin, S. Mifsud, L. Di Rago, D. Metcalf, M. Ernst, G. Dewson, A.W. Roberts, W.S. Alexander, J.M. Murphy, P.G. Ekert, S.L. Masters, D.L. Vaux, B.A. Croker, M. Gerlic, J. Silke, RIPK1 regulates RIPK3-MLKL-driven systemic inflammation and emergency hematopoiesis, Cell, 157 (2014) 1175-1188.
40. [40] X.N. Wu, Z.H. Yang, X.K. Wang, Y. Zhang, H. Wan, Y. Song, X. Chen, J. Shao, J. Han, Distinct roles of RIP1-RIP3 hetero- and RIP3-RIP3 homo-interaction in mediating necroptosis, Cell Death Differ, (2014).
41. [41] J. Li, U. Rix, B. Fang, Y. Bai, A. Edwards, J. Colinge, K.L. Bennett, J. Gao, L. Song, S. Eschrich, G. Superti-Furga, J. Koomen, E.B. Haura, A chemical and phosphoproteomic characterization of dasatinib action in lung cancer, Nat Chem Biol, 6 (2010) 291-299.
42. [42] D. Leveque, Pharmacokinetic interactions of dasatinib and docetaxel, Lancet Oncol, 15 (2014) e51.

Tables

Table 1
Phosphorylated Caspase-8 and clinical characteristics in patients with resectable lung adenocarcinoma (n=40)

	pY380-Casp8 n (%)		*P*
	Positive	Negative	
Age			
≤ 60	8 (44.4%)	6 (27.3%)	< 0.05
> 60	10 (55.6%)	16 (72.7%)	
Sex			
Male	12 (66.7%)	15 (68.2%)	> 0.05
Female	6 (33.3%)	7 (31.8%)	
Differentiation			
Well	3 (16.7%)	4 (18.2%)	> 0.05
Moderate	5 (27.8%)	5 (22.7%)	
Poor	10 (55.5%)	13 (58.8%)	
Lymphonode			
N_{0-1}	7 (38.9%)	9 (40.9%)	> 0.05
N_{2-3}	11 (61.1%)	13 (59.1%)	
pTNM			
I-II	4 (22.2%)	9 (40.9%)	< 0.05
III-	14 (77.8%)	13 (59.1%)	
Radiotherapy	12 (66.7%)	16 (72.7%)	> 0.05

Figures

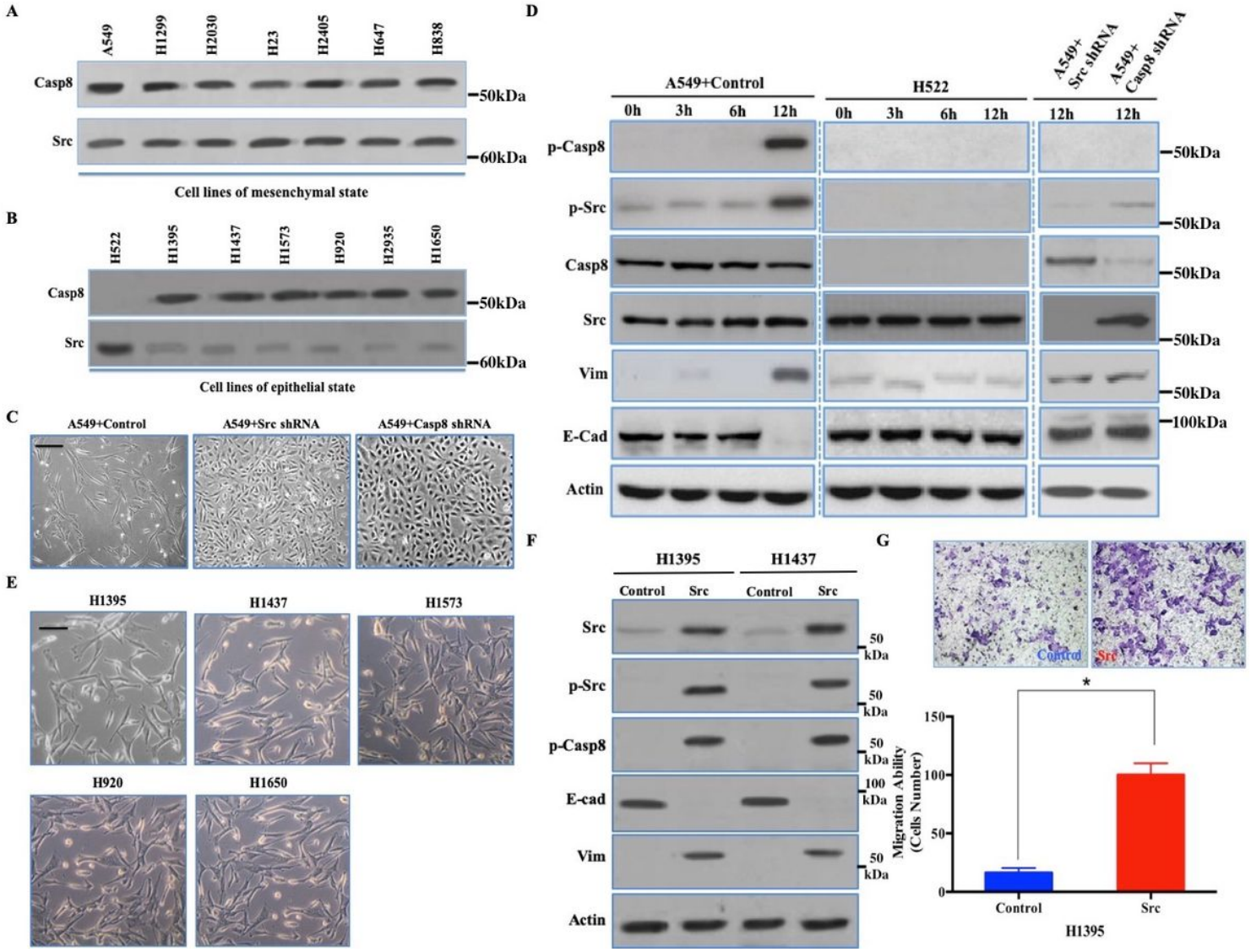

Figure 1

c-Src-induced Caspase-8 phosphorylation wasrequired for EMT in lung adenocarcinoma cell lines. A and B,Immunoblotting analysis of Caspase-8 and c-Src in the mesenchymal-like (A) (A549, H1299, H2030, H23, H2405, H647, H838)and epithelial-like (B) (H522, H1395, H1473, H1573, H920, H1650) lung adenocarcinoma cell lines plated onto fibronectin for 5 days. C, Phase contrast microscopy of A549 + Control/c-Src/Caspase-8 shRNA plated on dish coated with fibronectin over a 5-day period. Scale bars, 50 μm. D, Immunoblotting analysis of p-Casp8, p-Src, Caspase-8, c-Src, Vimentin, E-cadherin and β-actin in the A549 cells with control/c-Src/Caspase-8 shRNA and H522 cells plated onto fibronectin as indicated time. E, Phase contrast microscopy of H1395, H1473, H1573, H920, H1650 cells stably transfected with c-Srcplated on dish coated with fibronectin after a 5-day period. Scale bars, 50 μm. F, Immunoblotting analysis of c-Src, p-Src, p-Casp8, E-cadherin, Vimentin, and β-actin in H1395 and H1437 cells stably transfected with adenoviral control vector or c-Src plated onto fibronectin for 2 days. G, Transwell Boyden chamber analysis ofH1395 cells stably transfected with adenoviral control vector and c-Src. Mean ± SE from three determinations in a representative assay. *, p< 0.05.Scale bars, 50 μm.

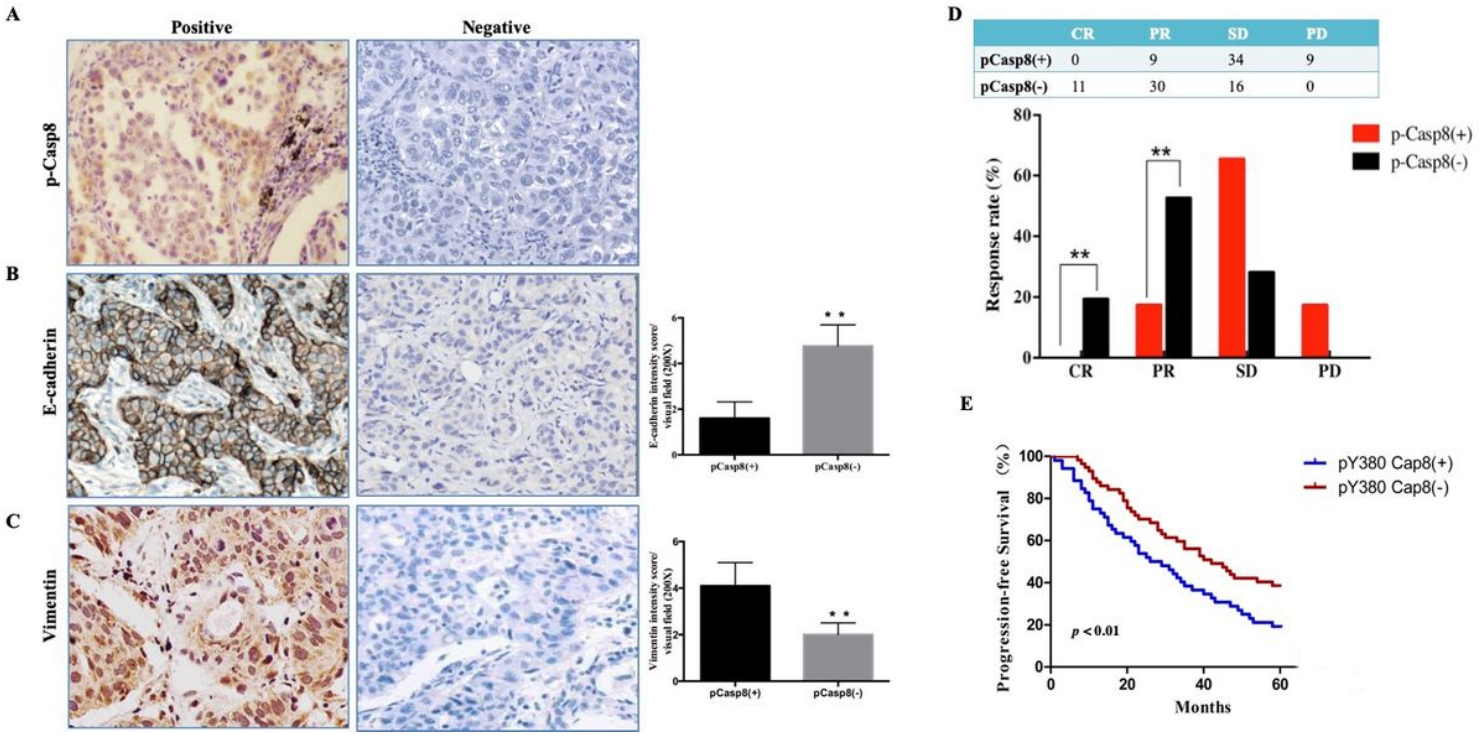

Figure 2

c-Src-induced Caspase-8 phosphorylation was associated with themesenchymal phenotype and contributed to chemoresistance in lung adenocarcinoma. A, B and CImmunohistochemical stainings for p-Casp8 (A), E-cadherin (B), Vimentin (C)with high magnification (×400).**, p< 0.01. Scale bar, 50μm. D, Response to cisplatin plus paclitaxel of patients withresectablelung adenocarcinoma. **, p< 0.01. E, Kaplan-MeirePFS curve for 109lung adenocarcinoma patientswith p-Casp8(+) or p-Casp8(-) following two neoadjuvant cycles of cisplatin and paclitaxel.p < 0.01.

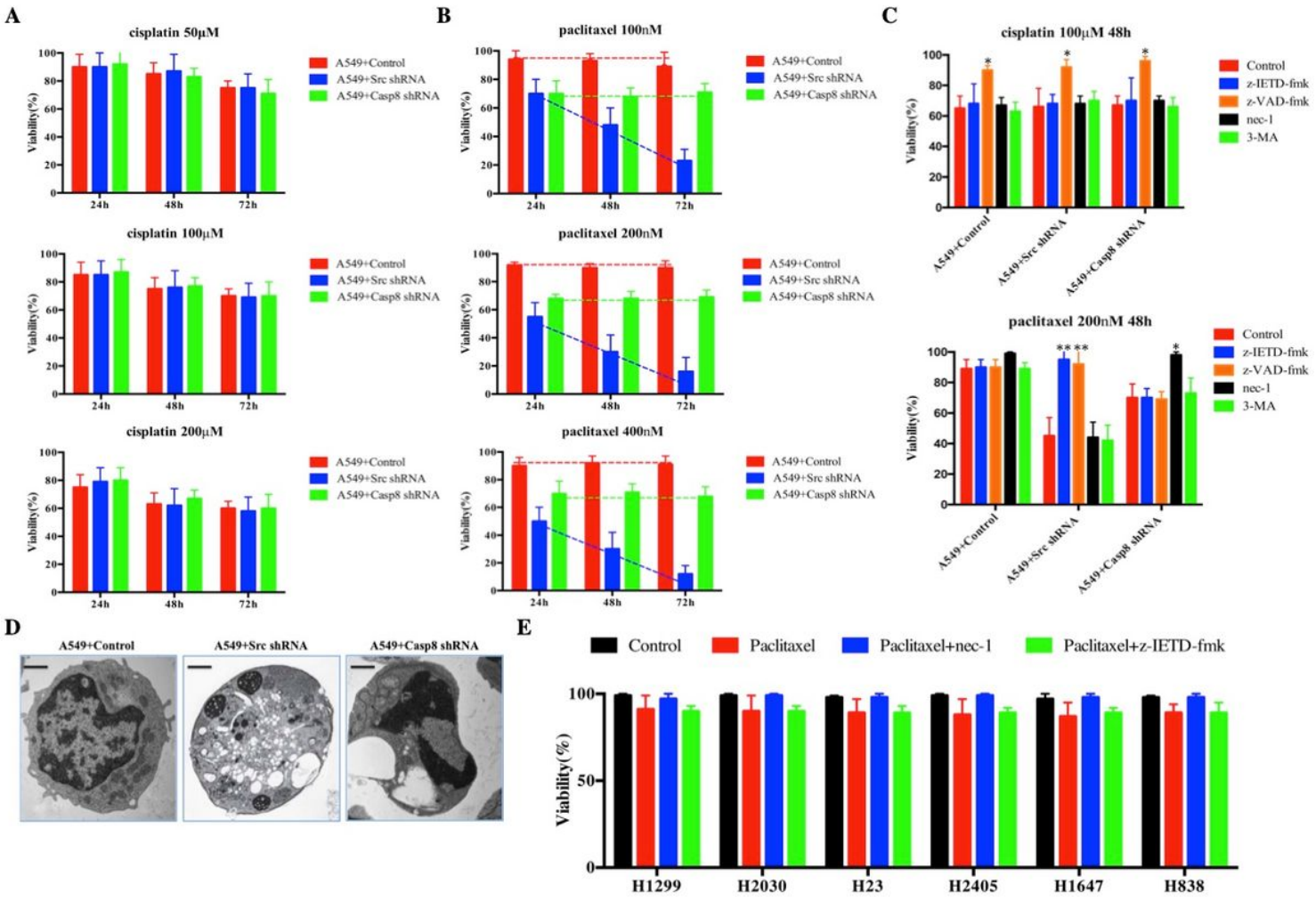

Figure 3

c-Src-mediated Caspase-8 phosphorylation inhibited cell death of lung adenocarcinoma through the paclitaxel-triggered necroptosis during EMT. A and B, A549 cells with Control/c-Src/Caspase-8 shRNA were treated with cisplatin (50/100/200 μM) (A) or paclitaxel (100/200/300 nM) (B) for 24, 48, 72hours. Cell viability was determined by measuring ATP levels using Cell Titer-Glo kit. Data were represented as mean ± standard deviation of duplicates. C, A549 cells with Control/c-Src/Caspase-8 shRNAwas treated with cisplatin (100 μM, upper) or paclitaxel (200 nM, lower) with the addition of DMSO (Control), zIETD-fmk (50 mM), zVAD-fmk (50 mM), nec-1 (10 mM), or 3-MA (25 mM) for 48 hours. Cell viability was determined by measuring ATP levels using Cell Titer-Glo kit. Data were represented as mean ± standard deviation of duplicates. *, $p< 0.05$, **, $p< 0.01$. D, Electron microscopy of A549 cells with Control/c-Src/Caspase-8 shRNA treated with paclitaxel for 48 h. Representative EM images were shown. E, Mesenchymal-like cell lines, H1299, H2030, H23, H2405, H1647, and H838 were treated with DMSO (Control), paclitaxel (200 nM), paclitaxel+nec-1 (10 mM), and paclitaxel+zIETD-fmk (50 mM)for 48 hours. Cell viability was determined by measuring ATP levels using Cell Titer-Glo kit. Data were represented as mean ± standard deviation of duplicates.

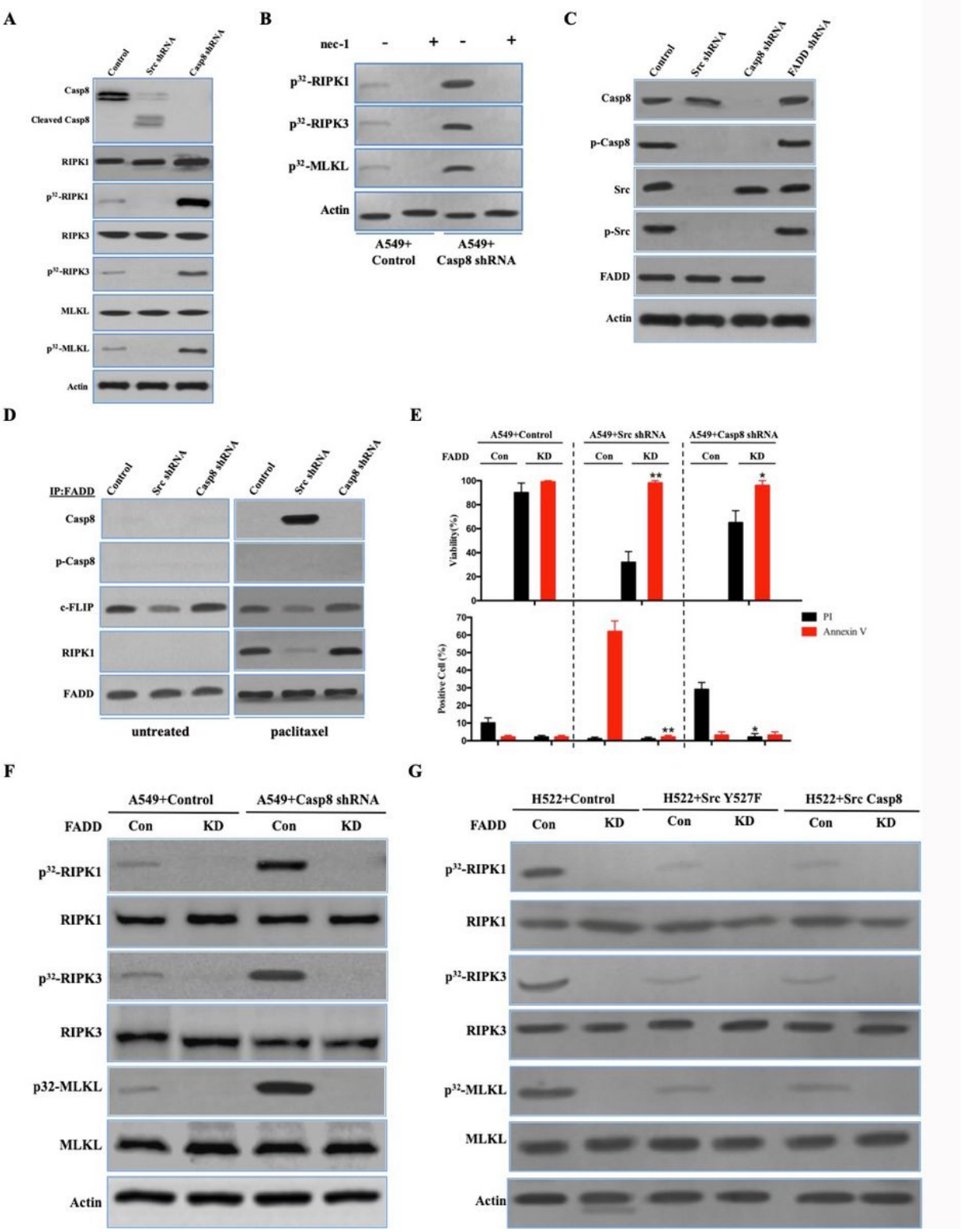

Figure 4

FADD interacted with Caspase-8, c-FLIP and RIPK1 to induce cell death signaling following paclitaxel treatment. A, Immunoblotting analysis of Caspase-8, cleaved Caspase-8, RIPK1, RIPK3, MLKL and β-actin in A549 cells with Control/c-Src/Caspase-8 shRNAtreated by 200nM paclitaxel for 48 hours after 48-hour attachment on the fibronectin-coated dish. Cells were labelled with [32P]-orthophosphate. Phosphorylated RIPK1, RIPK3 and MLKL were measured by Cyclone Plus Phosphor Imager. B, A549 cells with

Control/Caspase-8 shRNA were treated by 200nM paclitaxel with or without nec-1 for 48 hours after 48-hour attachment on the fibronectin-coated dish. Cells were labelled with [32P]-orthophosphate. Phosphorylated RIPK1, RIPK3 and MLKL were measured by Cyclone Plus Phosphor Imager. C, Immunoblotting analysis of Caspase-8, p-Casp8, c-Src, p-Src, FADD and β-actin in A549 cells with Control/c-Src/Caspase-8/FADD shRNAafter 48-hour attachment on the fibronectin-coated dish. D, The immunocomplexes of A549 cells with Control/c-Src/Caspase-8 shRNA treated with or without 200nM paclitaxel for 48 hours after 48-hour attachment on the fibronectin-coated dish were eluted with antibody against FADD, and whole elution was used to measure Caspase-8, p-Casp8, c-FLIP, and RIPK1. E,A549 cells with Control/ c-Src or Caspase-8 shRNAcombined with or without FADD knockdown were treated with 200 nM paclitaxel for 48 hours. Cell viability was determined by measuring ATP levels using Cell Titer-Glo kit. Data were represented as mean ± standard deviation of duplicates. Cells were analyzed for Annexin V/PI staining by flow cytometry. All experiments were repeated 3 times with similar results. *, vs. Control, $p < 0.05$. **, vs. Control, $p < 0.01$. F and G, Immunoblotting analysis of RIPK1, RIPK3, MLKL and β-actin in the A549 cells with Control/Caspase-8 shRNA (F) and H522 cells with Control/c-Src Y527F/Caspase-8 (G) combined with or without FADD knockdown after 48-hour attachment on the fibronectin-coated dish. Cells were labelled with [32P]-orthophosphate. Phosphorylated RIPK1, RIPK3 and MLKL were measured by Cyclone Plus Phosphor Imager.

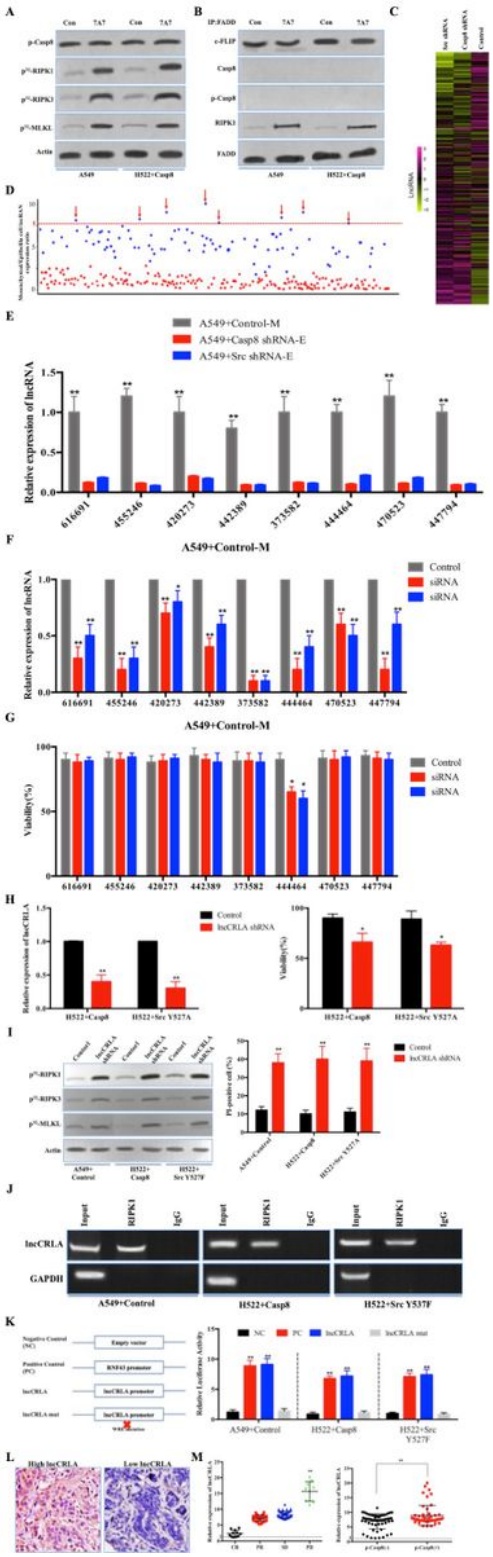

Figure 5

lncRNA-related chemotherapy resistance in lung adenocarcinoma (lncCRLA) inhibited RIPK1-induced necroptosis inthe mesenchymal-like lung adenocarcinoma. A, Immunoblotting analysis of p-Casp-8 and β-actin in the A549 cells and H522 cells with Caspase-8 treated by 200nM paclitaxel with or without 747 antibodyfor 48 hours after 48-hour attachment on the fibronectin-coated dish. Cells were labelled with [32P]-orthophosphate. Phosphorylated RIPK1, RIPK3 and MLKL were measured by Cyclone Plus

Phosphor Imager. B, The immunocomplexes of A549 cells and H522 cells with Caspase-8 treated by 200nM paclitaxel for 48 hours after 48-hour attachment on the fibronectin-coated dish were eluted with antibody against FADD, and whole elution was used to measure c-FLIP, Caspase-8, p-Casp8 and RIPK1. C, LncRNA microarray data of the mesenchymal-like (A549+Control) and the epithelial-like (A549+c-Src/Caspase-8 shRNA) cells was presented in a heatmap. D, Most differently expressedlncRNAs between mesenchymal-like (A549+Control) and epithelial-like(A549+c-Src/Caspase-8 shRNA) cells based on lncRNA microarray, > 8 folds. E, Verification of indicated lncRNAs in the mesenchymal-like (M) or epithelial-like (E) A549 cells by qRT-PCR (n = 3). F, Verification of interference efficiency of siRNAs for indicated lncRNAs in A549 cells with Control shRNA by qRT-PCR (n = 3). G, A549 cells with Control shRNAtransfected with indicated siRNAs were treated with 200 nM paclitaxel for 48 hoursafter 48-hour attachment on the fibronectin-coated dish. Cell viability was determined by measuring ATP levels using Cell Titer-Glo kit. Data were represented as mean ± standard deviation of duplicates.*, vs. Control, p< 0.05. H, qRT-PCR analysis of lncCRLA in H522 cells with c-Src Y527F/Caspase-8 stably transfected with controlor lncCRLA shRNA (left).Tumor cells as indicated were treated with 200 nM paclitaxel for 48 hours. Cell viability was determined by measuring ATP levels using Cell Titer-Glo kit (right). Data were represented as mean ± standard deviation of duplicates. *, vs. Control, p< 0.05.**, vs. Control, p< 0.01. I, Immunoblotting analysis ofβ-actin in A549 cells with Control shRNA and H522 cells with c-Src Y527F/Caspase-8 treated by 200nM paclitaxel for 48 hours after 48-hour attachment on the fibronectin-coated dish. Cells were labelled with [32P]-orthophosphate. Phosphorylated RIPK1, RIPK3 and MLKL were measured by Cyclone Plus Phosphor Imager (left).Cell viability was determined by measuring ATP levels using Cell Titer-Glo kit. Data were represented as mean ± standard deviation of duplicates (right).**, vs. Control, p< 0.01. J, RIP assay of the enrichment of RIPK1 on lncCRLA relative to IgG in the cytoplasmic lysates of A549 cells with Control shRNA and H522 cells with c-Src Y527F/Caspase-8 (n = 3). K, Luciferase activity analysis of a set of promoters as indicated transfected into A549 cells with Control shRNA and H522 cells with c-Src Y527F/Caspase-8. **, vs. Control, p< 0.01. L, LNA ISH analysis of lncCRLA with LNA probes in matched lung adenocarcinoma tissues. Representative LNA ISH images were shown. Scale bar, 50 μm. M, qRT-PCR analysis of lncCRLA in the patients with resectable lung adenocarcinoma with CR, PR, SD and PD during neoadjuvant chemotherapy (left). **, vs. CR, p< 0.01.qRT-PCR analysis of lncCRLA in the p-Casp8-positive or negativeresectable lung adenocarcinoma during neoadjuvant chemotherapy (right). **, p< 0.01.

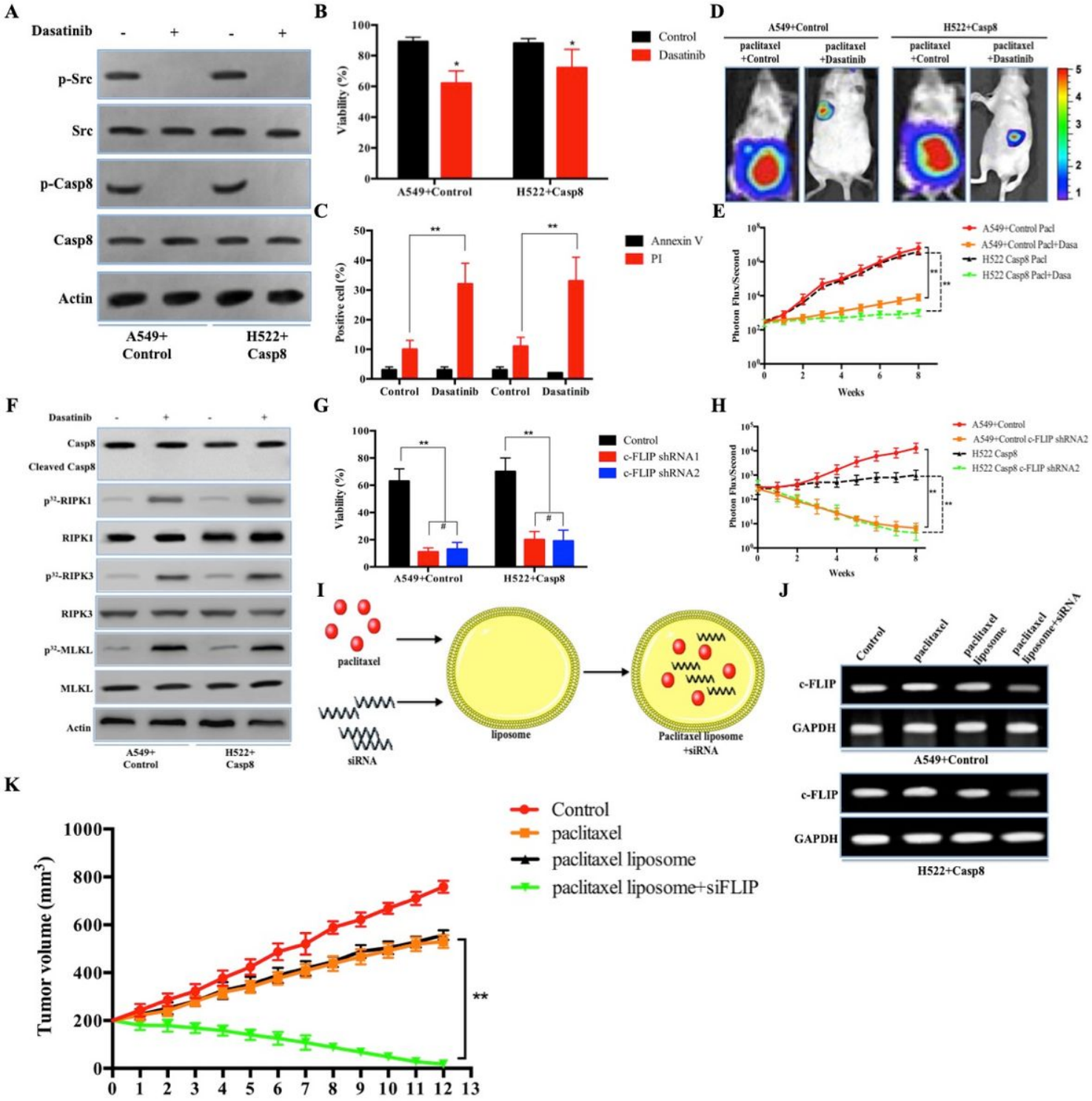

Figure 6

c-Src inhibitor,dasatinib and c-FLIP knockdown sensitized the mesenchymal-like lung adenocarcinoma cells to paclitaxel-induced cytotoxicity. A, Immunoblotting analysis of p-Src, c-Src, p-Casp8, Caspase-8 and β-actin in the A549 cells with Control shRNA and H522 cells with Caspase-8 treated by 200nM paclitaxel for 48 hours after 48-hour attachment on the fibronectin-coated dish. B, A549 cells with Control shRNA and H522 cells with Caspase-8were treated with 200 nM paclitaxel combined with or without dasatinib (20 nM) for 48 hoursafter 48-hour attachment on the fibronectin-coated dish. Cell viability was

determined by measuring ATP levels using Cell Titer-Glo kit. Data were represented as mean ± standard deviation of duplicates.*, vs. Control, p< 0.05. C, A549 cells with Control shRNA and H522 cells with Caspase-8were treated with 200 nM paclitaxel combined with or without dasatinib (20 nM) for 48 hoursafter 48-hour attachment on the fibronectin-coated dish. Cells were analyzed for Annexin V/PI staining by flow cytometry. All experiments were repeated 3 times with similar results. **, vs. Control, p< 0.01. D and E, Nude mice were subcutaneously xenografted with A549 cells with Control shRNA and H522 cells with Caspase-8 (1.0×106 cells) treated intravenously with paclitaxel plus oral vector or Dasatinib (n = 5 per group). Representative bioluminescent images (D), quantification of bioluminescent imaging signal intensities (E). **, vs. Control, p< 0.01. F, Immunoblotting analysis of Caspase-8, Cleaved Caspase-8, RIPK1, RIPK3, MLKL and β-actin in the A549 cells with Control shRNA and H522 cells with Caspase-8 treated by 200nM paclitaxel combined with or without Dasatinib (20 nM) for 48 hours after 48-hour attachment on the fibronectin-coated dish. G, A549 cells with Control shRNA and H522 cells with Caspase-8 stablytransfected with Control shRNA, c-FLIP shRNA1 and c-FLIP shRNA2 were treated with 200 nM paclitaxel combined with or without dasatinib (20 nM) for 48 hoursafter 48-hour attachment on the fibronectin-coated dish. Cell viability was determined by measuring ATP levels using Cell Titer-Glo kit. Data were represented as mean ± standard deviation of duplicates.**, vs. Control, p< 0.01. H, Nude mice were subcutaneously xenografted with A549 cells with Control shRNA and H522 cells with Caspase-8 stably transfected by c-FLIP shRNA2 (1.0×106 cells) treated with paclitaxel plus dasatinib (n = 5 per group). Quantification of bioluminescent imaging signal intensities. **, vs. Control, p< 0.01. I, Schematic diagram to illustrate the production of paclitaxel liposome+siFLIP. J, Gel electrophoresis of PCR products of lncCRLA and GAPDH in A549 cells with Control shRNA and H522 cells with Caspase-8 treated with control, paclitaxel, paclitaxel liposome and paclitaxel liposome+siFLIP for 48 hoursafter 48-hour attachment on the fibronectin-coated dish from qRT-PCR. K, Nude mice were subcutaneously xenografted with patient-derived tumors (5 mm in diameter) treated with oral dasatinib plus control, paclitaxel, paclitaxel liposome, paclitaxel liposome+siFLIP. **, p< 0.01.

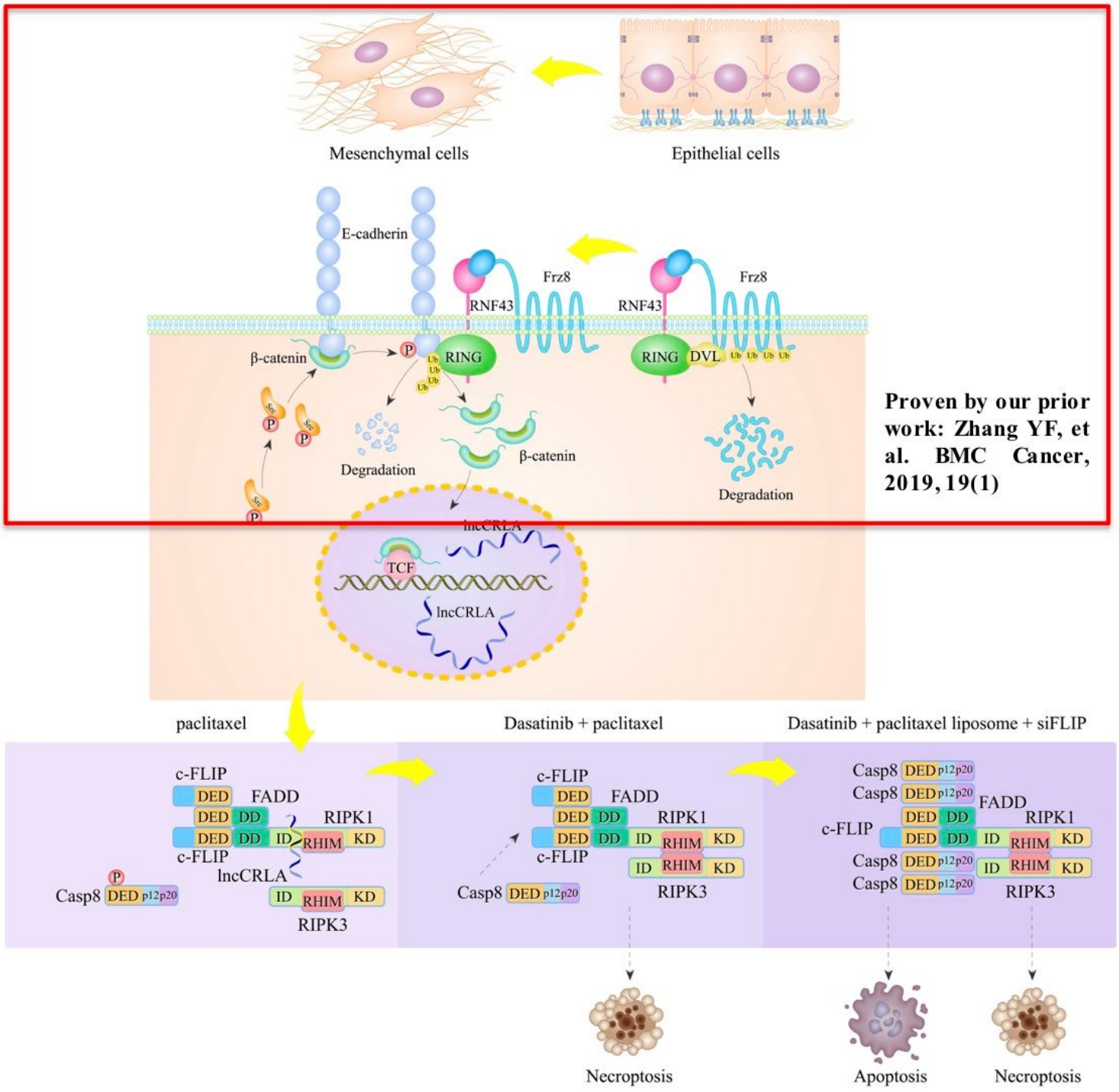

Figure 7

A schematic diagram of the resistance of the mesenchymal-like lung adenocarcinoma cells to paclitaxel.

Supplementary Files

This is a list of supplementary files associated with this preprint. Click to download.

- FigureS1.jpg
- FigureS1.jpg
- TableS1.docx
- TableS1.docx
- TableS3.xlsx
- TableS3.xlsx
- Supplementarymaterials.doc
- Supplementarymaterials.doc
- FigureS2.jpg
- FigureS2.jpg
- TableS2.docx
- TableS2.docx
- FigureS3.jpg
- FigureS3.jpg
- FigureS4.jpg
- FigureS4.jpg
- TableS4.xlsx
- TableS4.xlsx
- FigureS5.jpg
- FigureS5.jpg
- FigureS6.jpg
- FigureS6.jpg